Combination of a third generation bisphosphonate and replication-competent adenoviruses produces synergistic cytotoxicity on mesothelioma

（ビスフォスフォネート製剤と増殖性アデノウイルスの併用による胸膜中皮腫に対する抗腫瘍効果）

千葉大学大学院医学薬学府

先端医学薬学専攻

（主任：田川　雅敏 教授）

江　　媛媛

Abstract

Background: Approximately 80% of mesothelioma specimens have the wild-type *p53* gene, whereas they contain homozygous deletions in the INK4A/ARF locus that encodes $p14^{ARF}$ and the 16^{INK4A}. We examined whether zoledronic acid (ZOL), a third generation bisphosphonate, and adenoviruses with a deletion of the *E1B-55kD* gene (Ad-delE1B55), which augments p53 levels in the infected tumors, could produce possible combinatory anti-tumor effects on human mesothelioma cells bearing the wild-type *p53* gene.

Methods: Cytotoxicity of ZOL and Ad-delE1B55 was assessed with a WST assay. Cell cycle changes were tested with flow cytometry. Expression levels of relevant molecules were examined with western blot analysis to analyze a possible combinatory mechanism. Furthermore, the expressions of Ad receptors on target cells and infectivity were investigated with flow cytometry. Viral replications were examined with the tissue culture infection dose method.

Results: Synergistic cytotoxic effects were produced by ZOL and Ad-delE1B55 on mesothelioma. Sub-G1 and S-phase populations increased compared with a single treatment of ZOL or Ad-delE1B55. The combinatory treatment induced p53 phosphorylation and subsequently enhanced the cleavage of caspase-3, 8, 9 and poly (ADP-ribose) polymerase, but did not influence expression of molecules involved in autophagy pathways. The Ad infectivity and replication of Ad-delE1B55 was stronger in the combination than those without ZOL treatment although the expression levels of Ad receptors remained unchanged.

Conclusions: These findings indicated that combination of ZOL and Ad-delE1B55 induce synergistic anti-tumor effects through apoptotic pathways.

Keywords: malignant mesothelioma; replication-competent adenovirus; bisphosphonates.

Introduction

Malignant pleural mesothelioma, developed in the pleural cavity, is highly related to exposure to asbestos in the patient history [1,2]. Approximately 80% of mesothelioma showed homozygous deletions in the INK4A/ARF locus which encodes $p14^{ARF}$ and the 16^{INK4A} but the *p53* was infrequently mutated [3,4]. The prognosis remains poor despite recent therapeutic modalities, and a novel therapeutic strategy is required to improve the survival.

Bisphosphonates (BPs) are synthetic analogues of pyrophosphates and strongly show affinity for mineralized bone matrix [5]. Recent reports showed that BPs had cytotoxic activities on tumors such as breast and prostate cancer [6,7], and these cytotoxic actions were attributable to a number of mechanisms including apoptosis induction and anti-angiogenesis [8, 9]. Zoledronic acid (ZOL), one of the third generation BPs, inhibits the farnesyl pyrophosphate synthetase, a key enzyme in the mevalonate pathway, and depletes isoprenoid pools, which subsequently results in decreased prenylation of small guanine-nucleotide-binding regulatory proteins (small G proteins). Consequently, ZOL prevented growth, adhesion or spreading, and invasion of cancer cells [5,10]. In our previous study, we investigated ZOL-mediated cytotoxic effects on mesothelioma cells [11]. Furthermore, ZOL treatments improved cytotoxicity of adenoviruses (Ad) expressing the *p53* gene on mesothelioma, showing that ZOL-mediated augmentation of p53 was essential in the combinatory effects with a p53 up-regulating agent [12].

Replicating Ad is a new strategy for cancer therapy. They can spread and destroy tumors without deleterious effects in normal tissues [13]. Replication-competent Ad continuously release the progenies from infected tumors and consequently circumvent low transduction efficacy. This replicable propensity enhances the cytotoxicity although host immunity is inhibitory to the viral spreading. Ad lacking the E1B-55kDa molecules (Ad-delE1B55) are replication-competent and were originally hypothesized to target only *p53*-mutated or -null tumors due to the defect in p53-inactivating E1B-55 kDa protein [14]. However, Ad proteins synthesized during the replications regulate p53 expression at various levels even in an epigenetic manner [15]. Ad-delE1B55-induced cytotoxicity was related to accumulation of p53 phosphorylation. Additionally, our previous study showed that Ad-delE1B55 produced cytotoxicity on mesothelioma cells in a combination with the first- line chemotherapeutic agents [16].

In the present study, we examined whether ZOL and Ad-delE1B55 could produce combinatory anti-tumor effects on human mesothelioma cells carrying the wild-type *p53* gene. Furthermore, we indicated that combinatory effects were induced through apoptotic pathways.

Material and methods

Cells

Human mesothelioma cells, MSTO-211H, NCI-H28 and NCI-H226, which were purchased from American Type Culture Collection (Manassas, VA, USA), were cultured with RPMI 1640 medium with 10% fetal calf serum. HEK 293 and A549 cells (provided from Dr. Katsutyuki Hamada, Ehime University, Japan) were cultured with in Dulbecco's Modified Eagle's Medium containing 10% fetal calf serum.

Ad preparation

Replication-competent Ad-delE1B55, in which the 55kDa molecule-encoding E1B region is deleted, and replication-incompetent Ad expressing the *ß-galactosidase* (Ad-LacZ) or the g*reen fluorescent protein* gene (Ad-GFP) powered by the cytomegalovirus promoter, were prepared with an Adeno-X expression system (Takara, Shiga, Japan) and HEK293 cells. The numbers of virus particles (vp) per ml was estimated with the formula [absorbance at 260 nm of purified Ad in the presence of 0.1 % sodium dodecyl sulfate.

Cell cycle analysis

Cells were fixed in ice-cold 100% ethanol, incubated with RNase (50 μg/ml) and stained with propidium iodide (50 μg/ml). The staining profiles were analyzed with FACSCalibur and CellQuest software (BD Biosciences, CA, USA).

Viability test in vitro

Cells (5 x 10^3/well) seeded in 96-well plates cultured with ZOL (Novartis, Basel, Switzerland), Ad-delE1B55 or ZOL plus Ad-delE1B55 for 5 days. Cell viability was determined with a cell-counting WST kit (Wako, Osaka, Japan) and the relative viability was calculated based on the absorbance without any treatments. Viable cell numbers were also counted with the trypan blue dye exclusion test. Combinatory effects were examined with CalcuSyn software (Biosoft, Cambridge, UK). Combination index (CI) values at respective fractions affected (Fa) points, which showed relative suppression levels of cell viability, were calculated based on the WST assay. CI < 1, CI = 1 and CI > 1 indicate synergistic, additive and antagonistic actions, respectively.

Western blot analysis

Cells were cultured with ZOL and/or Ad and the cell lysate was subjected to sodium dodecyl sulfate polyacrylamide gel electrophoresis. The protein was transferred to a nylon filter and was hybridized with antibodies (Ab), against p53 (Thermo Fisher Scientific, Fremont, CA, USA),

phosphorylated p53 at serine (Ser) 15, Bid, caspase-3, cleaved caspase-3, caspase-8, cleaved caspase-8, caspase-9, cleaved caspase-9, poly (ADP-ribose) polymerase (PARP), Beclin-1, Atg5, LC3A/B (Cell Signaling, Danvers, MA, USA), type 2/5 Ad E1A (Santa Cruz Biotech, Dallas, TX, USA), phosphorylated H2AX at Ser 139 (Biolegend, San Diego, CA, USA), and α-tubulin (Thermo Fisher Scientific) as a control. The membranes were developed with the ECL system (GE Healthcare, Buckinghamshire, UK).

Infectivity with Ad-GFP and expression of Ad receptors

Cells were infected with Ad-GFP at a certain vp dose for 30 min and were then washed to remove Ad. Infected cells were cultured for 2 days and then analyzed for percentages of GFP-positive cells with FACSCalibur (BD Biosciences) and CellQuest software (BD Biosciences). Cells of which fluorescence was greater than the brightest 5% of uninfected cells were judged as positively stained. For detecting Ad receptors, cells were stained with anti-coxsackie adenovirus receptors (CAR) (Upstate, Charlottesville, VA, USA), integrin αvβ3 (Chemicon, Billerica, MA, USA), integrin αvβ5 (Abcam, Cambrige, UK) and the fluorescence intensity was analyzed with FACSCalibur and CellQuest software.

Virus production

Cells lysate after Ad infection was examined for the cytotoxicity with A549 cells and the virus titers were calculated with the median tissue culture infectious dose ($TCID_{50}$) method.

Results

Cytotoxic activities of ZOL and Ad-delE1B55 on mesothelioma

We investigated possible combinatory cytotoxic effects produced by ZOL and Ad-delE1B55 on 5 kinds of mesothelioma, MSTO-211H, NCI-H226, NCI-H28, EHMES-10 and NCI-H2452 cells, which are defective of the $p14^{ARF}$ and $p16^{INK4A}$ genes but possess the wild-type *p53* (Figure 1). Cells treated with ZOL or Ad-delE1B55 showed decreased viability. A combinatory use of both ZOL and Ad-delE1B55 achieved cytotoxicity greater than a single treatment with either ZOL or Ad-delE1B55 (Figure 2A). CalcuSyn software analyses showed that CI values were below 1 in MSTO-211H, NCI-H226 and NCI-H28 cells at most of the Fa points tested, indicating that the combination of ZOL and Ad-delE1B55 achieved synergistic cytotoxicity. We also calculated live cell numbers of combination-treated cells (Figure 2B). Cell growth was gradually retarded, and the cell numbers reduced stronger in the combination than those treated with ZOL or Ad-delE1B55. Replication-incompetent Ad-LacZ minimally suppressed the proliferation. These data indicated that ZOL and Ad-delE1B55 induced growth arrest and produced synergistic cytotoxic effects on mesothelioma.

Cell cycle changes induced by ZOL and Ad- delE1B55

We examined cell cycle changes with flow cytometry in MSTO-211H and NCI-H28 cells (Figure 3; Table 1 and 2). Ad-delE1B55 treatments increased hyperploid fractions, more than 4N populations, and sub-G1 fractions and ZOL increased sub-G1 fractions in MSTO-211H cells (Figure 3A). A combinatory used further increased sub-G1 populations in comparison with treatments with of Ad-delE1B55 or ZOL alone. Induction of hyperploidy was greater in NCI-H28 cells than in MSTO-211H cells when they were infected with Ad-delE1B55, and ZOL minimally augmented S-phase populations in NCI-H28 cells (Figure 3B). Combination of both agents in NCI-H28 cells induced the same cell cycle changes that were produced by Ad-delE1B55 treatments. In contrast to MSTO-211H cells, combination treatment did not induce Sub-G1 but increased S-phase fractions probably because Ad-delE1B55–infected cells with hyperploid fractions did not enter into G2/M-phase but still stayed in G2-phase. Cells uninfected or infected with Ad-LacZ however showed a minimal level of polyploidy and Sub-G1 fractions did not increase markedly.

Molecular changes induced by combination of ZOL and Ad-delE1B55

We examined a possible mechanism of combination effects produced by ZOL and Ad-delE1B55 with western blot analyses (Figure 4). We firstly detected viral gene *E1A* expression in MSTO-211H cells (Figure 4A). E1A became detectable at 24 hours after infection of Ad-delE1B55, but the levels were minimally different compared with the combination

treatment. We then examined expression levels of apoptosis-linked proteins (Figure 4B). MSTO-211H cells treated with both ZOL and Ad-delE1B55 showed up-regulated p53 expression, p53 phosphorylation, and subsequently enhanced cleavage of caspase-3, 8, 9 and PARP at a greater level than those treated with ZOL or Ad-delE1B alone. We noticed that Bid expression was down-regulated after 96 hours, but truncated Bid, which contributes to the linkage between the death receptor- and the mitochondria-mediated apoptosis, was not induced. Interestingly, phosphorylation of H2AX, a marker of DNA damages, was augmented suggesting that DNA damages were involved in Ad-delE1B55-mediated cell death and the combination augmented the damages.

We also examined a possible involvement of autophagy pathways (Figure 4A). Beclin-1 or Atg5 expression did not show any enhancement and there was no transition from LC3A/B I to LC3A/B II accompanied by the combination. These data indicated that cell death induced by ZOL and Ad-delE1B was irrelevant to autophagy.

Expression of Ad receptors and Ad infectivity with mesothelioma cells.

We examined expression level changes of CAR and integrin αvβ3 or αvβ5 molecules induced by ZOL treatment on 2 kinds of mesothelioma cells (Figure 5A). The expression levels expressed as mean fluorescent intensity were calculated as a percentage of untreated cells and ZOL did not influence the CAR (MSTO-211H; 108.2 ± 0.09, NCI-H28 cells; 100.63 ± 0.39) or αvβ3 (MSTO-211H; 100.7 ± 0.04, NCI-H28 cells; 97.9 ± 0.37) expression levels. In contrast, ZOL differentially affect the integrin αvβ5 expression levels (MSTO-211H; 115.9 ± 0.64, NCI-H28 cells (69.7 ± 0.2). We then tested Ad infectivity on mesothelioma using GFP-expressing Ad with flow cytometry (Figure 5B). The fluorescence intensity on NCI-H28 cells was influenced by ZOL, but not on MSTO-211H cells. These results suggested that the Ad infectivity of Ad-delE1B55 was stronger in the combination than that without ZOL treatment although the expression levels of Ad receptors did not change.

The effects of ZOL on viral proliferations of Ad-delE1B55.

We examined whether the enhanced combinatory effects were associated with increased production of the viral progenies by ZOL treatment. MSTO-211H and NCI-H28 cells were treated with ZOL and Ad-delE1B55, then the cell lysate was tested for the viral titers with the $TCID_{50}$ method with A549 cells (Figure 6). There was no change in 211H cell, but ZOL treatment significantly suppressed viral propagation of Ad-delE1B55. The enhanced cell death by the combination was not thereby due to increased production of infectious Ad progenies on MSTO-211H cells, but could be linked with a new mechanism by ZOL that could influence Ad-delE1B55 replication on mesothelioma.

Discussion

In this study, we firstly examined that ZOL and Ad-delE1B55 induced growth arrest and produced synergistic cytotoxic effects on *p53* wild-type mesothelioma. Sub-G1 populations increased compared with a single treatment of ZOL or Ad-delE1B55 in MSTO-211H cells. However, the combination in NCI-H28 cells did not induce Sub-G1 but increased S-phase populations. The mechanism of S-phase arrest induced by the combinatory treatment remain uncharacterized. The combinatory treatment induced p53 phosphorylation and subsequently enhanced the cleavage of caspase-3, 8, 9 and PARP, but did not influence expression of molecules implicated in autophagy pathways. H2AX was also phosphorylated, which suggested that a cellular system detecting viral DNA increase during the replications was activated. Hyperploidy could be due to a direct or an indirect consequence of accumulated viral DNA and an activated DNA damage sensor thereby phosphorylated H2AX molecules. However, it is currently unknown as for a precise mechanism of the combinatory effects on mesothelioma.

The majority of human mesothelioma possesses the wild type *p53* gene but lacks the $p14^{ARF}$ and the 16^{INK4A} genes, which subsequently disorganized the p53 and the pRb pathways, respectively. ZOL activated p53 pathways on mesothelioma even though the cell death did not depend on the p53 pathways in our recent study [10]. On the other hand, Ad-delE1B55 that produced cytotoxicity on mesothelioma induced in p53 phosphorylation, pRb dephosphorylation, and cleavage of caspases [16]. The present study indicated that combination phosphorylated p53 and up-regulated the expression levels, suggesting a crucial role of p53 induction in the combination-mediated cytotoxicity.

The ZOL-induced cytotoxicity can be attributable to inhibited prenylation of small G proteins and showed a possible involvement of the p53 pathways in ZOL-mediated cytotoxicity [5, 8,9]. Ras and RhoA pathways were activated on malignant mesothelioma and extracellular-regulated kinase 1/2, p38 mitogen-activated protein kinase, and c-Jun N-terminal kinase were found to be active in most of the mesothelioma cell lines tested [11, 17]. Cell death caused by Ad-delE1B55 was associated with activated p53 pathways [18]. The combinatory effects were therefore associated with a possible cross-talk between small G proteins and the p53 pathways on mesothelioma.

We examined expression of Ad receptors and the Ad infectivity on mesothelioma cells. CAR and integrin αvβ3 expression levels on MSTO-211H and NCI-H28 cells were minimally different in ZOL-treated cells. Intriguingly, integrin αvβ5 expression was augmented in MSTO-211H and down-regulated in NCI-H28 cells after ZOL treatments although contribution of the differential expression to the Ad infectivity were unknown. By contrast, Ad replication of Ad-delE1B55 was stronger in the combination than that in ZOL treatment on NCI-H28 cells. These results suggested a possible mechanism connected with sub-G1 increase and S-phase

arrest which induced by the combinatory treatment. Ad replication processes are not directly associated with hyperploidy, but that differential cell death mechanisms, which are influenced by a number of genetic differences in infected cells, may also play a role in the aberrant cell cycle progression [19]. On the other hand, some studies showed that cells infected with Ad-delE1B55 during the G1 phase of cell cycle exhibited a reduced rate of viral late protein synthesis, produced fewer viral progeny, and were less efficiently killed than cells infected during the S-phase [20, 21]. Therefore, S-phase arrest which induced on NCI-H28 cells could enhance viral progeny

We also hypothesized a possible mechanism involved in the combinatory effects with small G proteins interactions between ZOL and Ad. Ad endocytosis via integrins requires activation of the lipid kinase phosphatidylinositol-3-OH kinase, which in turn augments signaling cascades of both Ras and Rho families [22]. In addition, our previous study showed that RhoA, Cdc42 and Rab6 were achievable targets for ZOL-induced actions [23]. These reports suggested that combinatory cytotoxicity of ZOL and Ad-delE1B55 was linked with small G proteins functions, however, precise interactions remained unknown. Our studies demonstrated synergistic anti-tumor effects induced by combination of ZOL and Ad-delE1B55 through multiple mechanisms.

Conclusions

In this study, we examined ZOL and Ad-delE1B55 induced growth arrest and produced synergistic cytotoxic effects on *p53* wild-type mesothelioma. We showed that the combination of ZOL and Ad-delE1B55 ~~i~~nduced synergistic anti-tumor effects through apoptotic pathways. The interrelationship of small G proteins and the p53 pathways also play a role associated with the cell death on mesothelioma.

Abbreviations

Ab: antibody; Ad: adenoviruses; Ad-delE1B55: Ad lacking the E1B-55kDa molecules; BPs: Bisphosphonates; CAR: coxsackie adenovirus receptor; CI: combination index; Fa: fractions affected; GFP: green fluorescent protein; H2AX: H2A histone family member X; LacZ: ß-galactosidase; MOI: multiplicity of infection; PARP: poly (ADP-ribose) polymerase; PI3K: lipid kinase phosphatidylinositol-3-OH kinase; pfu: plaque-forming unit; small G proteins: mall guanine-nucleotide-binding regulatory proteins; $TCID_{50}$: median tissue culture infectious dose; vp: virus particles; ZOL: zoledronic acid.

References

1. Favoni RE, Florio T. Combined chemotherapy with cytotoxic and targeted compounds for the management of human malignant pleural mesothelioma. Trends Pharmacol Sci. 2011;32:463-79.
2. Carbone M, Kratzke RA, Testa JR. The pathogenesis of mesothelioma. Semin Oncol. 2002; 29:2-17.
3. Hopkins-Donaldson S, Belyanskaya LL, Simões-Wüst AP, Sigrist B, Kurtz S, Zangemeister-Wittke U, et al. p53-induced apoptosis occurs in the absence of p14(ARF) in malignant pleural mesothelioma. Neoplasia. 2006;8:551-9.
4. Lee AY, Raz DJ, He B, Jablons DM. Update on the molecular biology of malignant mesothelioma. Cancer. 2007;109:1454-61.
5. Yuasa T, Kimura S, Ashihara E, Habuchi T, Maekawa T. Zoledronic acid: a multiplicity of anti-cancer action. Curr Med Chem. 2007;14:2126-35.
6. Lee MV, Fong EM, Singer FR, Guenette RS. Bisphosphonate treatment inhibits the growth of prostate cancer cells. Cancer Res. 2001;61:2602-8.
7. Senaratne SG, Pirianov G, Mansi JL, Arnett TR, Colston KW. Bisphosphonates induce apoptosis in human breast cancer cell lines. Br J Cancer. 2000;82:1459-68.
8. Green JR. Antitumor effects of bisphosphonates. Cancer. 2003;97:840-7.
9. Green JR. Bisphosphonates: preclinical review. Oncologist. 2004;9:3-13.
10. Jones RM., Morgan C, Bertelli G. Effects of zoledronic acid and docetaxel on small GTP-binding proteins in prostate cancer. Tumor Biol. 2015;36:4861-9.
11. Okamoto S, Kawamura K, Li Q, Yamanaka M, Yang S, Fukamachi T, et al. Zoledronic acid produces antitumor effects on mesothelioma through apoptosis and S-phase arrest in p53-independent and Ras prenylation-independent manners. J Thorac Oncol. 2012;7:873-82.
12. Okamoto S, Jiang Y, Kawamura K, Shingyoji M, Fukamachi T, Tada Y, et al. Zoledronic acid produces combinatory anti-tumor effects with Cisplatin on mesothelioma by increasing p53 expression levels. PLoS One. 2013;8(3): e60297.
13. Yang CT, You L, Uematsu K, Yeh CC, McCormick F, Jablons DM. p14(ARF) modulates the cytolytic effect of ONYX-015 in mesothelioma cells with wild-type p53. Cancer Res. 2001;61:5959-63.
14. Bischoff JR, Kirn DH, Williams A, Heise C, Horn S, Muna M, et al. An adenovirus mutant that replicates selectively in p53-deficient human tumor cells. Science. 1996;274:373-376.
15. Soria C, Estermann FE, Espantman KC, O'Shea CC. Heterochromatin silencing of p53 target genes by a small viral protein. Nature. 2010;466:1076-81.

16. Yamanaka M, Tada Y, Kawamura K, Li Q, Okamoto S, Chai K, et al. E1B-55 kDa-defective adenoviruses activate p53 in mesothelioma and enhance cytotoxicity of anticancer agents. J Thorac Oncol. 2012;7:1850-7.
17. Patel MR, Jacobson BA, De A, Frizelle SP, Janne P, Thumma SC, et al. Ras pathway activation in malignant mesothelioma. J Thorac Oncol. 2007;2:789-95.
18. Bar-Sagi D, Hall A. Ras and Rho GTPases: a family reunion. Cell. 2000;103:227-38.
19. Yang S, Kawamura K, Okamoto S, Yamauchi S, Shingyoji M, Sekine I, et al. Cytotoxic effects of replication-competent adenoviruses on human esophageal carcinoma are enhanced by forced p53 expression. BMC Cancer. 2015;15:464.
20. Goodrum FD, Ornelles DA. Roles for the E4 orf6, orf3, and E1B 55-kilodalton proteins in cell cycle-independent adenovirus replication. J Virol. 1999;73:7474-88.
21. Goodrum FD, Ornelles DA. The early region 1B 55-kilodalton oncoprotein of adenovirus relieves growth restrictions imposed on viral replication by the cell cycle. J Virol. 1997;71:548-61.
22. Li E, Stupack D, Bokoch GM, Nemerow GR. Adenovirus endocytosis requires actin cytoskeleton reorganization mediated by Rho family GTPases. J Virol. 1998;72:8806-12.
23. Okamoto S, Jiang Y, Kawamura K, Shingyoji M, Tada Y, Sekine I, et al. Zoledronic acid induces apoptosis and S-phase arrest in mesothelioma through inhibiting Rab family proteins and topoisomerase II actions. Cell Death Dis. 2014; doi:10.1038, e1517.

Table 1. Cell cycle progressions of MSTO-211H cells treated with ZOL and/ or Ad-delE1B55.

Cells	Time (hr)	Treatment	Cell cycle distribution (%±SE)				
			Sub-G1	G1	S	G2/M	>4N
MSTO-211H	24	(-)	2.04±0.04	58.80±0.20	18.17±0.24	20.67±0.31	0.81±0.06
		Ad-LacZ	2.90±0.16	57.30±0.19	17.59±0.22	20.97±0.26	1.83±0.04
		Ad-delE1B55	2.61±0.16	55.29±0.07	20.41±0.11	20.08±0.27	2.22±0.11
		ZOL	2.47±0.05	57.47±0.10	18.34±0.27	20.70±0.22	1.62±0.09
		ZOL+ Ad-LacZ	3.58±0.17	55.98±0.16	17.94±0.17	20.84±0.10	2.22±0.08
		ZOL+ Ad-delE1B55	3.72±0.05[a]	53.99±0.11[a]	20.53±0.23[a]	19.42±0.35	3.00±0.09
	48	(-)	1.73±0.07	76.54±0.12	8.20±0.03	12.59±0.08	1.18±0.04
		Ad-LacZ	1.37±0.08	75.90±0.38	8.60±0.16	12.55±0.33	1.82±0.03
		Ad-delE1B55	12.25±0.04	51.87±0.21	12.47±0.13	21.56±0.19	2.32±0.03
		ZOL	3.82±0.08	76.77±0.43	6.70±0.09	11.31±0.33	1.60±0.01
		ZOL+ Ad-LacZ	2.81±0.11	76.08±0.33	7.47±0.12	11.95±0.13	1.96±0.06
		ZOL+ Ad-delE1B55	19.69±0.18[a]	47.47±0.19[a]	15.42±0.44[a]	15.23±0.35	2.69±0.16
	72	(-)	0.96±0.02	87.55±0.01	3.77±0.13	7.26±0.19	0.59±0.05
		Ad-LacZ	1.46±0.10	87.58±0.30	2.75±0.05	7.79±0.14	0.51±0.03
		Ad-delE1B55	22.52±0.07	43.47±0.18	11.57±0.14	12.89±0.23	10.14±0.23
		ZOL	11.19±0.08	76.77±0.28	3.45±0.08	7.93±0.20	0.81±0.12
		ZOL+ Ad-LacZ	6.44±0.03	80.27±0.15	3.04±0.04	9.66±0.13	0.78±0.04
		ZOL+ Ad-delE1B55	35.52±0.05[a]	24.06±0.30[a]	13.89±0.13[a]	11.83±0.21[b]	15.41±0.19
	96	(-)	1.03±0.07	87.25±0.01	4.43±0.03	6.93±0.06	0.50±0.03
		Ad-LacZ	1.16±0.06	87.36±0.28	3.34±0.17	7.65±0.11	0.68±0.04
		Ad-delE1B55	12.14±0.27	53.92±0.29	11.93±0.06	13.21±0.27	9.32±0.31
		ZOL	9.32±0.11	80.72±0.21	3.98±0.06	5.73±0.07	0.40±0.07
		ZOL+ Ad-LacZ	8.93±0.17	78.40±0.17	4.22±0.14	7.92±0.13	0.79±0.04
		ZOL+	40.75±0.08[a]	21.50±0.21[a]	14.26±0.11	10.58±0.12	13.59±0.18[b]

Ad-delE1B55

Cells were treated with ZOL or Ad-delE1B55 ($4.5x10^3$ vp/cell) and compared with no treated or Ad-LacZ ($4.5x10^3$ vp/cell) and cultured for 24-96 hours.

Cell cycle profiles were analyzed with flow cytometry. Mean percentages with SEs are shown (n=3).

[a] $p < 0.01$, [b] $p < 0.05$; compared between ZOL+Ad-delE1B55-treated cells, and Ad-LacZ, ZOL-, Ad-delE1B55-, ZOL+Ad-LacZ-treated cells.

Table 2. Cell cycle progressions of NCI-H28 cells treated with ZOL and/ or Ad-delE1B55.

Cells	Time (hr)	Treatment[a]	Cell cycle distribution (%±SE)[b]				
			Sub-G1	G1	S	G2/M	>4N
NCI-H28	24	(-)	8.57±0.34	57.61±1.07	15.48±0.53	16.96±0.89	0.92±0.21
		Ad-LacZ	0.17±0.02	58.59±0.71	18.33±0.19	22.24±0.39	1.18±0.17
		Ad-delE1B55	0.25±0.10	59.35±0.68	20.28±0.08	15.33±0.38	5.45±0.19
		ZOL	0.16±0.03	61.76±0.64	25.71±0.31	212.15±0.48	0.89±0.05
		ZOL+ Ad-LacZ	0.15±0.03	67.62±0.48	21.85±0.35	9.87±0.20	0.96±0.07
		ZOL+ Ad-delE1B55	0.23±0.03	65.45±0.73[a]	17.33±0.21[a]	14.21±0.38[a]	3.24±0.24[a]
	48	(-)	2.79±0.15	7.58±0.13	9.30±0.05	13.66±0.20	0.93±0.06
		Ad-LacZ	0.24±0.01	73.42±0.15	9.22±0.21	16.30±0.20	1.08±0.13
		Ad-delE1B55	1.17±0.05	1.70±0.22	8.77±0.22	36.84±0.12	51.80±0.28
		ZOL	0.86±0.10	58.00±0.54	25.64±0.15	15.28±0.27	0.82±0.11
		ZOL+ Ad-LacZ	0.70±0.03	60.80±0.20	25.40±0.27	12.92±0.28	0.77±0.03[c]
		ZOL+ Ad-delE1B55	1.44±0.22[a]	19.93±1.20	47.98±1.01[a]	1.28±0.32[a]	0.64±0.37[a]
	72	(-)	1.06±0.02	76.33±0.64	9.26±0.23	12.68±0.28	0.92±0.21
		Ad-LacZ	0.51±0.06	76.20±0.37	8.68±0.26	13.50±0.46	1.41±0.07
		Ad-delE1B55	6.67±0.17	2.15±0.23	5.12±0.49	27.45±0.26	59.21±0.85
		ZOL	5.67±0.23	59.46±0.21	19.55±0.57	14.86±0.47	1.02±0.07
		ZOL+ Ad-LacZ	6.07±0.13	61.94±0.30	16.93±0.16	14.56±0.12	0.97±0.11
		ZOL+ Ad-delE1B55	8.56±0.38[a]	7.77±0.84[a]	41.33±1.20[a]	22.49±0.42	20.77±0.11[a]

Cells were treated with ZOL or Ad-delE1B55 ($4.5x10^3$ vp/cell) and compared with no treated or Ad-LacZ ($4.5x10^3$ vp/cell) and cultured for 24-96 hours.

Cell cycle profiles were analyzed with flow cytometry. Mean percentages with SEs are shown (n=3).

[a] $p < 0.01$; compared between ZOL+Ad-delE1B55-treated cells, and Ad-LacZ, ZOL-, Ad-delE1B55-, ZOL+Ad-LacZ-treated cells.

Figure legends

Figure 1 Cytotoxic activities of ZOL or Ad-delE1B55 in mesothelioma.

(A) Cells were treated with ZOL for 5 days and the cell viabilities were measured with the WST assay. The relative viabilities were calculated based on the absorbance without any treatments. Means of triplicated samples and SE bars are shown (n = 3). (B) Cells were infected with various amounts of Ad-delE1B55 and the viability was tested with the WST assay 5 days after the infection. Relative viability was calculated based on uninfected cells. Averages and SE bars are shown (n = 3).

Figure 2 Combinatory effects produced by ZOL and Ad-delE1B55.

(A) Cells were treated with different doses of ZOL and Ad-delE1B55 for 5 days and the cell viabilities were measured with the WST assay. Means of triplicated samples and the SE bars are shown (n=3). CI values based on the cell viabilities were determined by different Fa points with CalcuSyn software. (B) Cell proliferation were determined with the trypan blue dye exclusion test. SEs are shown. *$p < 0.01$, compared ZOL plus Ad-delE1B55-treated group with Ad-LacZ, ZOL-, Ad-delE1B55-, ZOL plus Ad-LacZ-treated cells group.

Figure 3 Representative profiles of cell-cycle analyses.

MSTO-211H (A) or NCI-H28 cells (B) were treated with ZOL and Ad-delE1B55 or Ad-LacZ (MSTO-211H: 4.5×10^3 vp/cell; NCI-H226: 1×10^3 vp/cell), and the cell cycles were analyzed with flow cytometry.

Figure 4 Expression of molecules linked with cell death by combinatory treatment.

MSTO-211H cells were treated with ZOL and Ad-delE1B55 or Ad-LacZ (3×10^3 vp/cell) as a control. Cells were cultured for the indicated times. Expression of viral proteins and autophagy pathways (A) and molecules linked with cell death pathways (B) were examined with western blot analyses.

Figure 5 Expressions of Ad receptors and infectivity of Ad.

(A) Expression of CAR and integrin αvβ3 or αvβ5 molecules in MSTO-211H and NCI-H28 cells analyzed with flow cytometry. Representative profiles of cells untreated or treated with ZOL are shown. The thin line shows the mean fluorescent intensity of unstain cells and the thick line shows the mean fluorescent intensity of stain cells. (B) ZOL-mediated infection efficacy examined with Ad-GFP. Cells were infected at different MOI of Ad and mean fluorescent intensity of the GFP-positive cells are indicated. Averages and the SE bars are shown (n = 3).

Figure 6 Viral replications with the combination.

Influence of ZOL on viral proliferation of Ad-delE1B55. MSTO-211H and NCI-H28 cells were treated with Ad-delE1B55 or in combination of ZOL (MSTO-211H: Ad-delE1B55 3×10^3 vp/cell, ZOL 10 μM; NCI-H28: Ad-delE1B55 1×10^3 vp/cell, ZOL 50 μM) and the cell lysate was extracted at the indicated times. The viral titers were assayed with the TCID50 method. Means and SE bars are shown (n = 3).

Figure 1

A

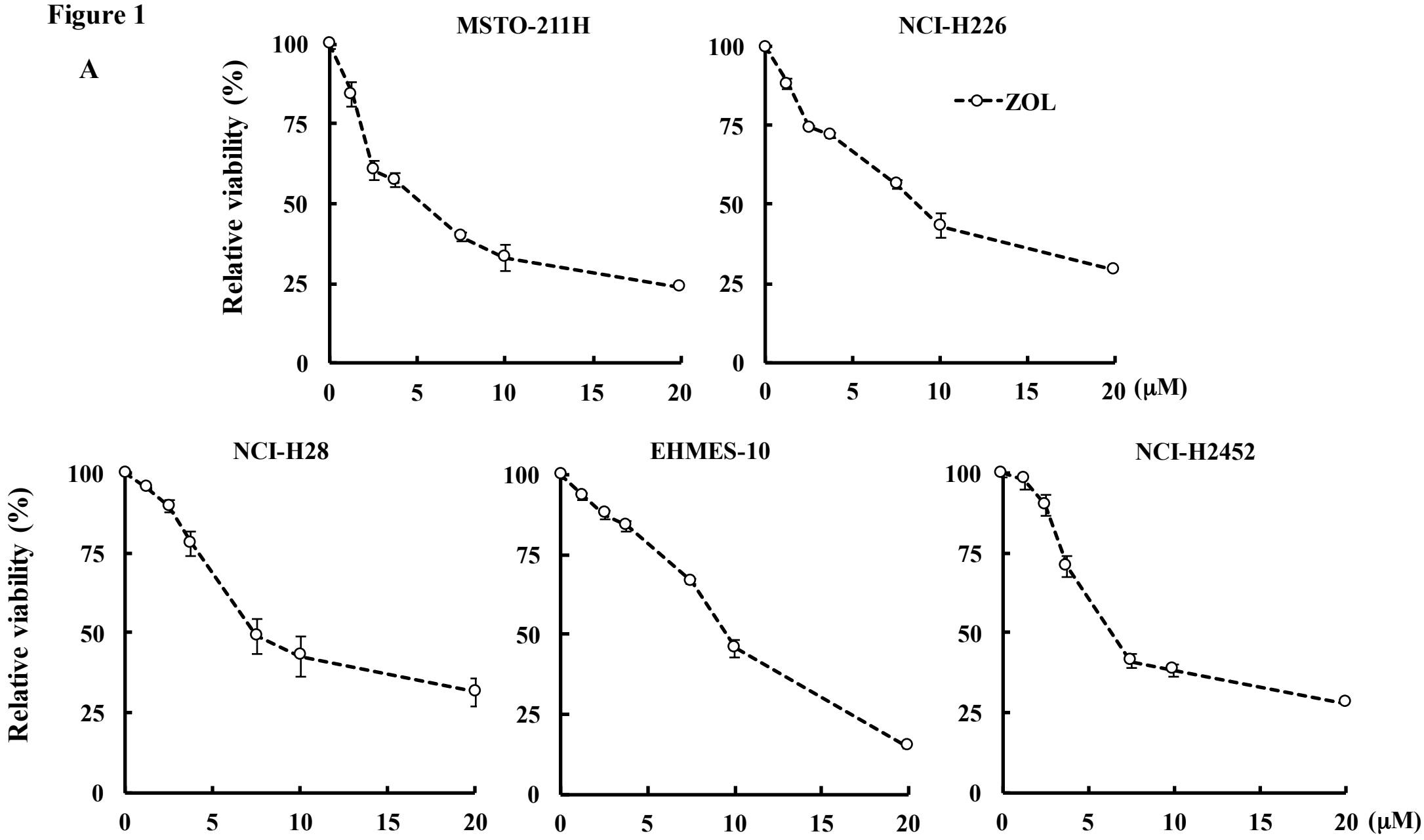
MSTO-211H
NCI-H226
ZOL
Relative viability (%)
100
75
50
25
0
0
5
10
15
20
(μM)
NCI-H28
EHMES-10
NCI-H2452

B

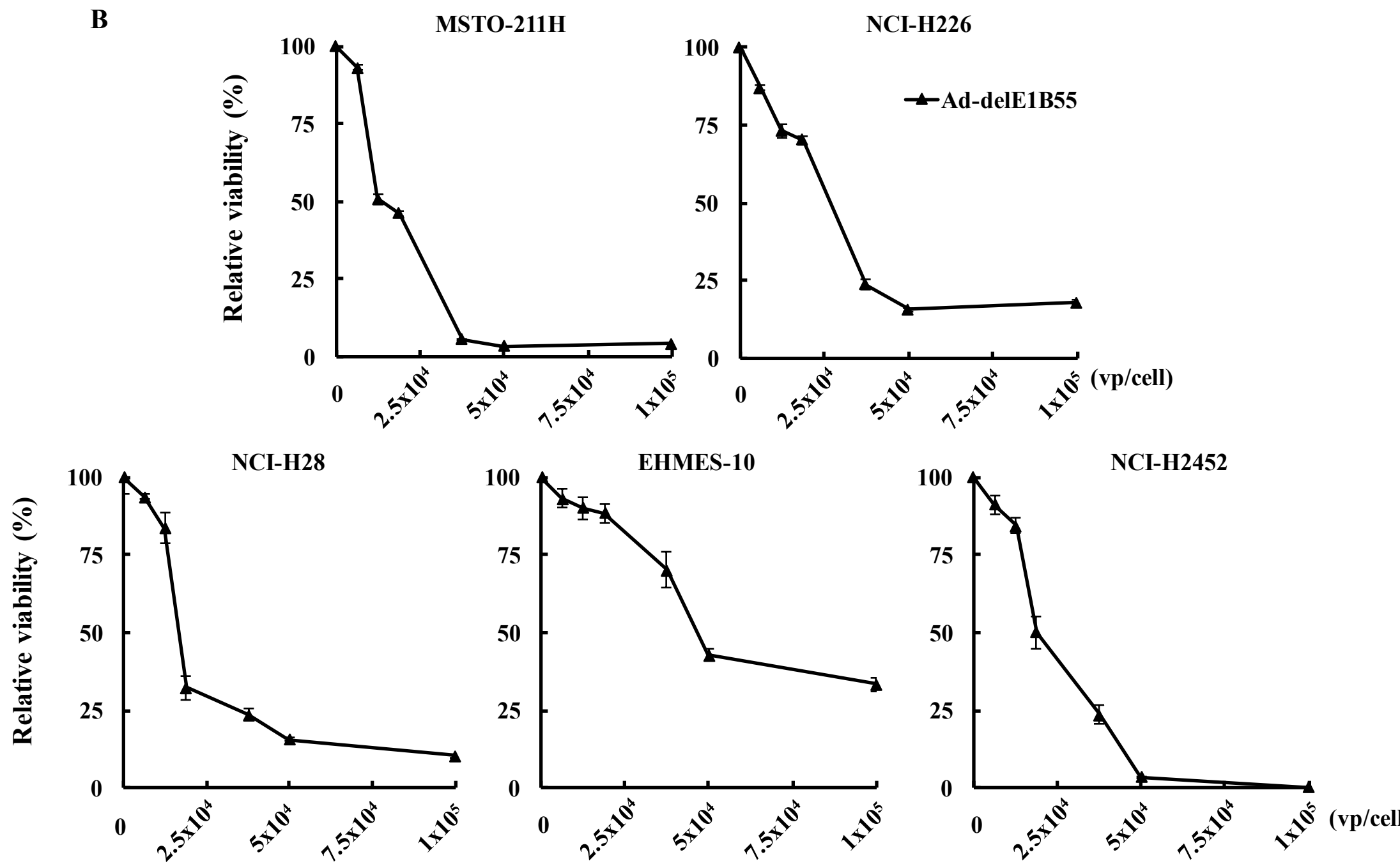
MSTO-211H
NCI-H226
Ad-delE1B55
Relative viability (%)
100
75
50
25
0
0
2.5x10⁴
5x10⁴
7.5x10⁴
1x10⁵
(vp/cell)
NCI-H28
EHMES-10
NCI-H2452

Figure 2

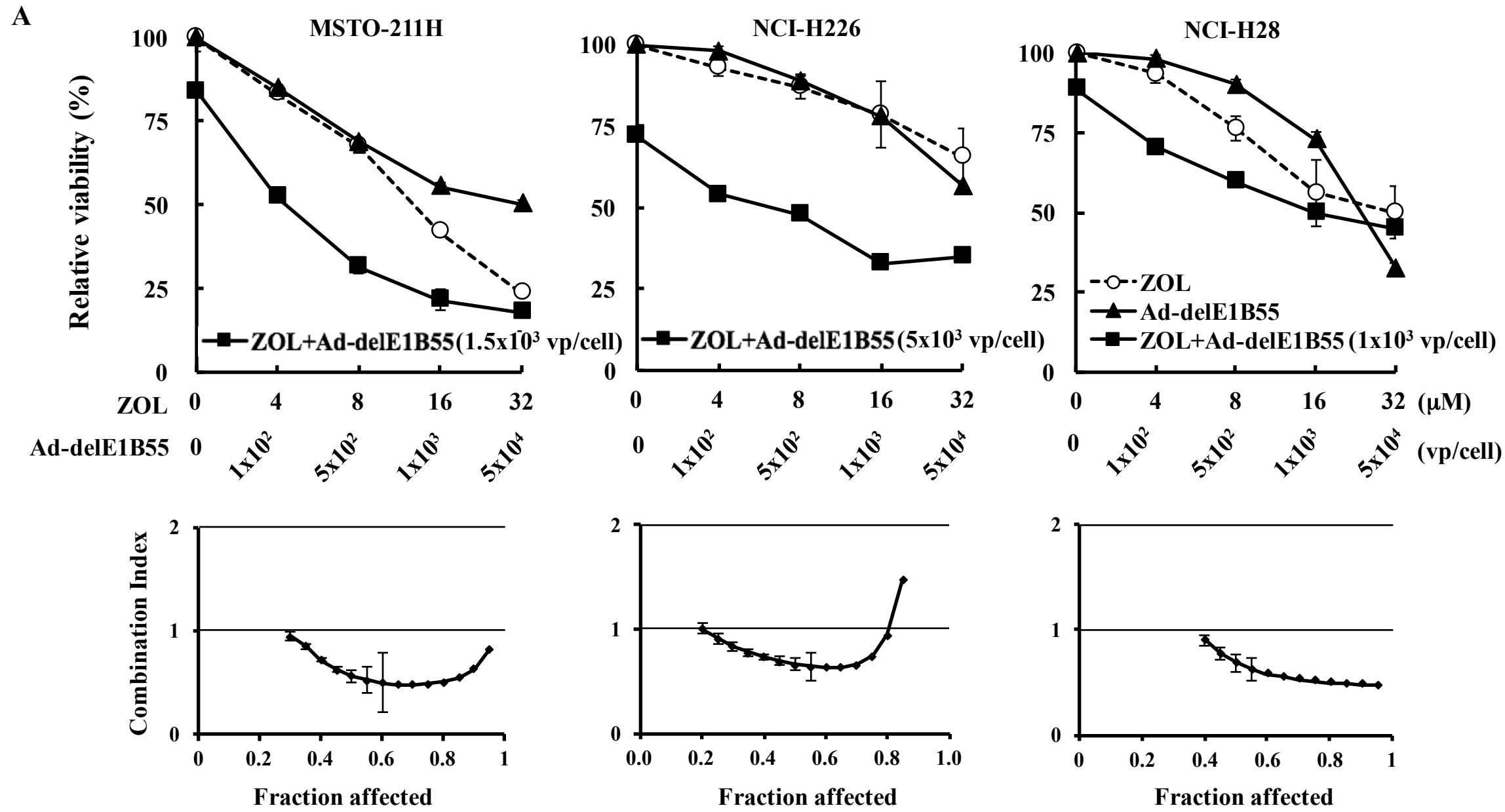
A
MSTO-211H
NCI-H226
NCI-H28
Relative viability (%)
ZOL+Ad-delE1B55 (1.5x10³ vp/cell)
ZOL+Ad-delE1B55 (5x10³ vp/cell)
ZOL+Ad-delE1B55 (1x10³ vp/cell)
ZOL
Ad-delE1B55
ZOL 0 4 8 16 32 (μM)
Ad-delE1B55 0 1x10² 5x10² 1x10³ 5x10⁴ (vp/cell)
Combination Index
Fraction affected

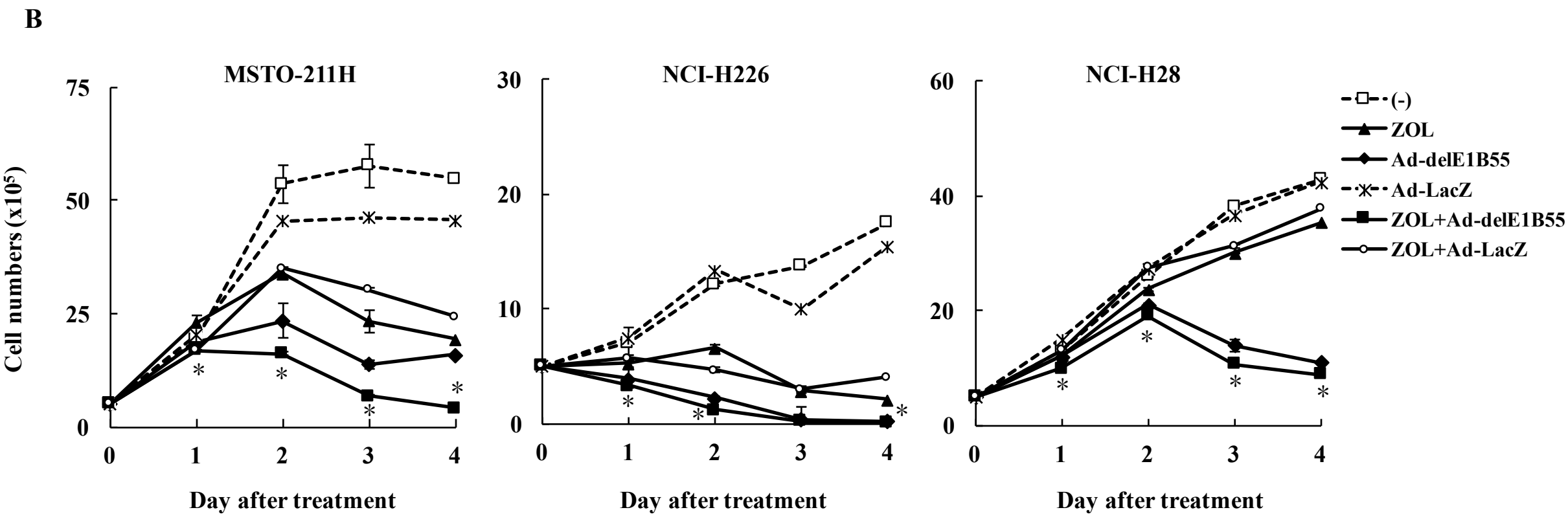
B
MSTO-211H
NCI-H226
NCI-H28
Cell numbers (x10⁵)
(-)
ZOL
Ad-delE1B55
Ad-LacZ
ZOL+Ad-delE1B55
ZOL+Ad-LacZ
Day after treatment

Figure 3

A

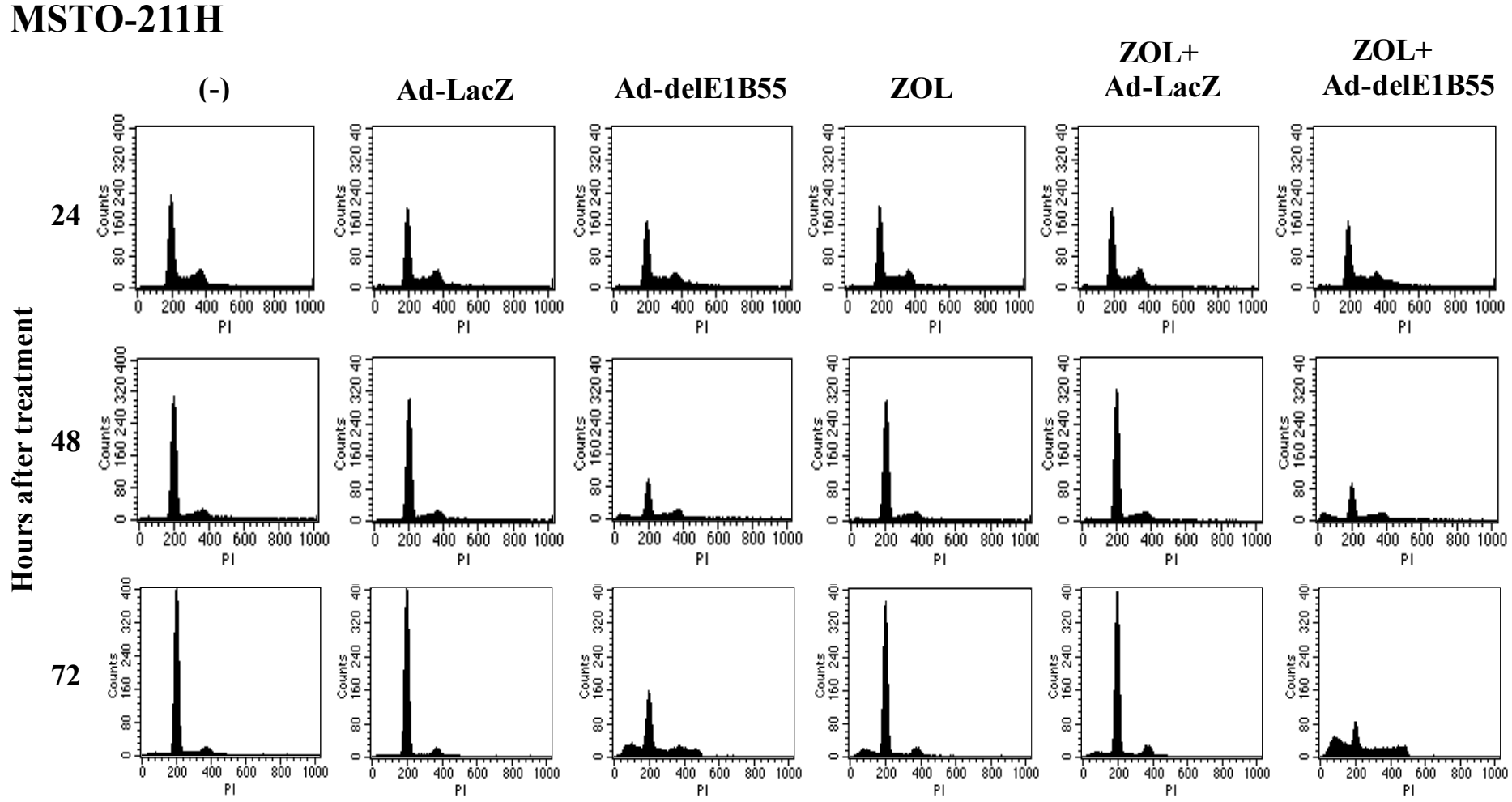
MSTO-211H
(-)
Ad-LacZ
Ad-delE1B55
ZOL
ZOL+ Ad-LacZ
ZOL+ Ad-delE1B55
Hours after treatment
24
48
72
Counts
PI

B

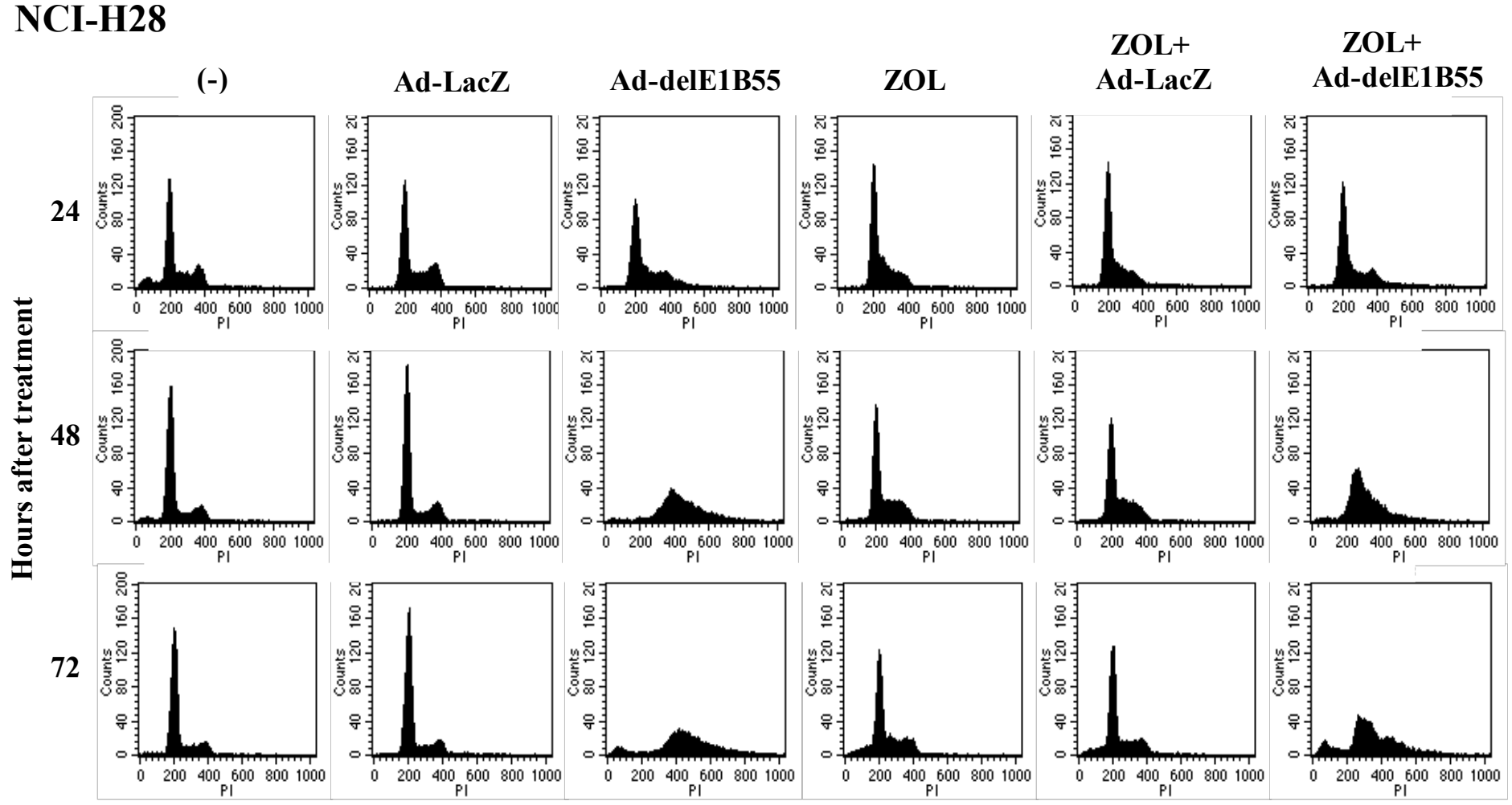
NCI-H28
(-)
Ad-LacZ
Ad-delE1B55
ZOL
ZOL+ Ad-LacZ
ZOL+ Ad-delE1B55
Hours after treatment
24
48
72
Counts
PI

Figure 4

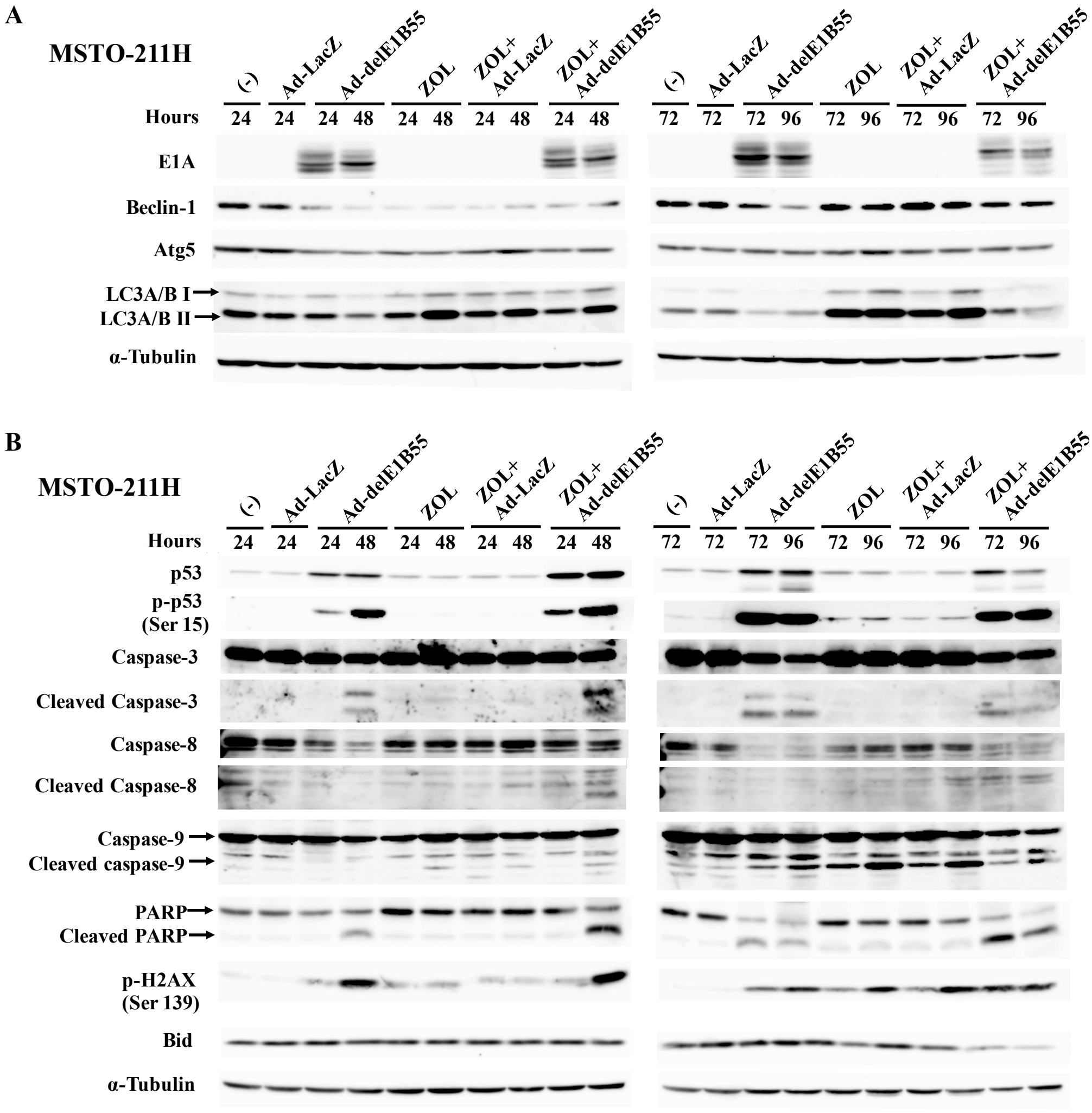
A
MSTO-211H
(-)
Ad-LacZ
Ad-delE1B55
ZOL
ZOL+ Ad-LacZ
ZOL+ Ad-delE1B55
Hours
24 24 24 48 24 48 24 48 24 48
72 72 72 96 72 96 72 96 72 96
E1A
Beclin-1
Atg5
LC3A/B I
LC3A/B II
α-Tubulin
B
MSTO-211H
p53
p-p53 (Ser 15)
Caspase-3
Cleaved Caspase-3
Caspase-8
Cleaved Caspase-8
Caspase-9
Cleaved caspase-9
PARP
Cleaved PARP
p-H2AX (Ser 139)
Bid
α-Tubulin

Figure 5

A

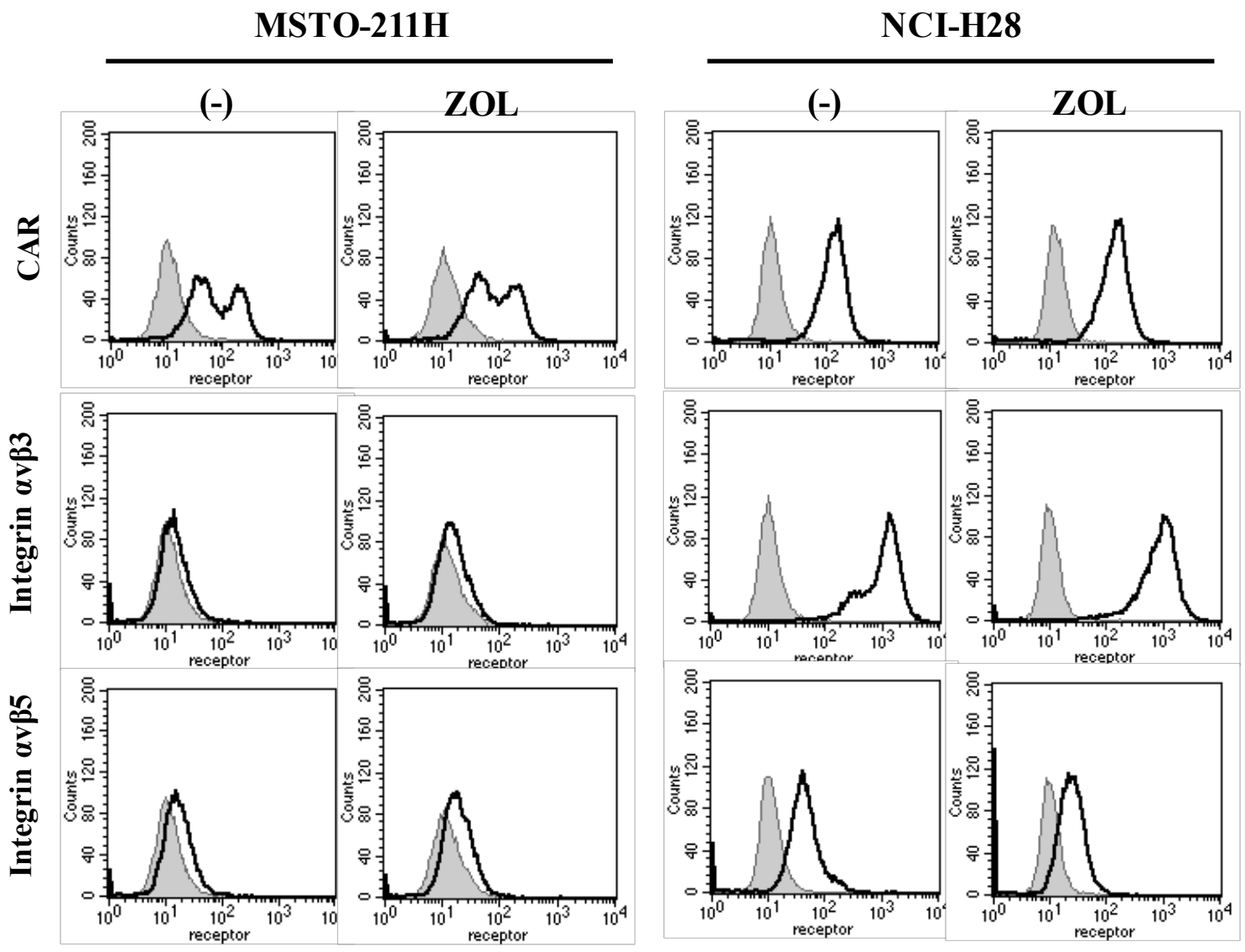
MSTO-211H
NCI-H28
(-)
ZOL
CAR
Integrin αvβ3
Integrin αvβ5
Counts
receptor

B

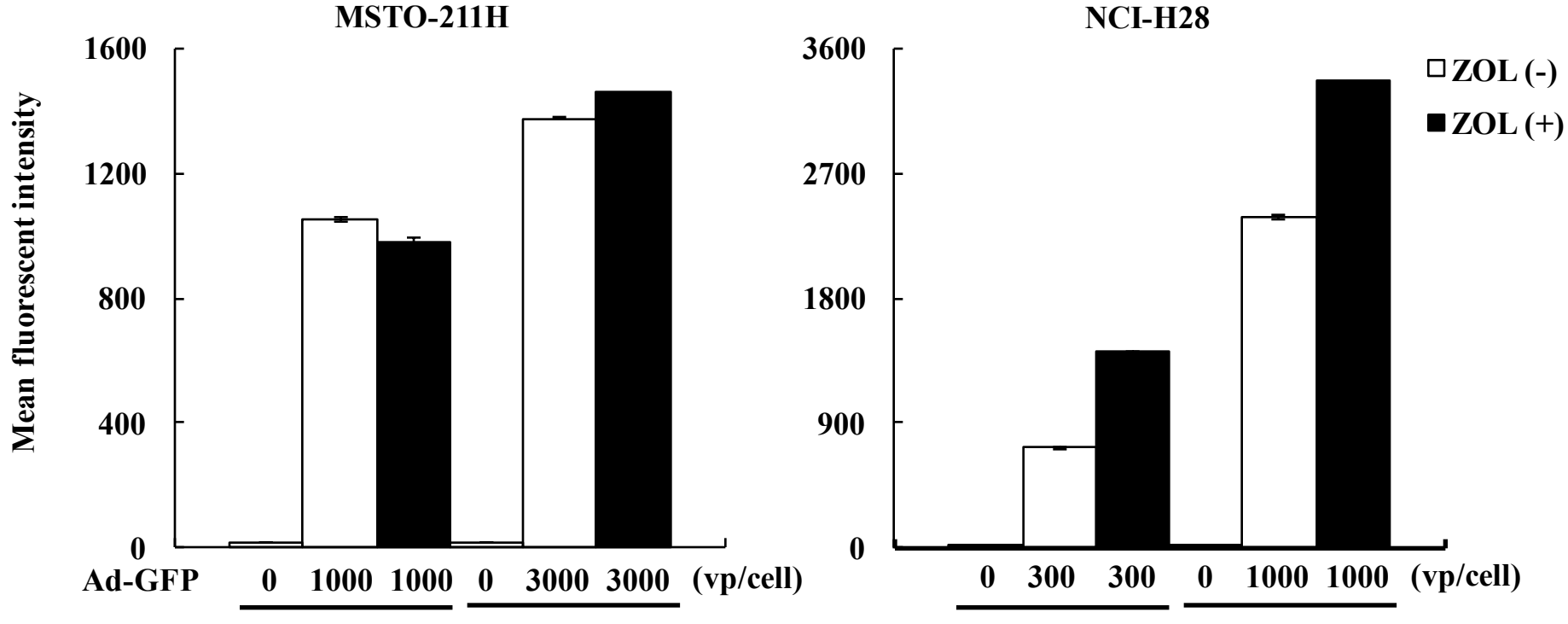
MSTO-211H
NCI-H28
Mean fluorescent intensity
ZOL (-)
ZOL (+)
Ad-GFP
(vp/cell)

Figure 6

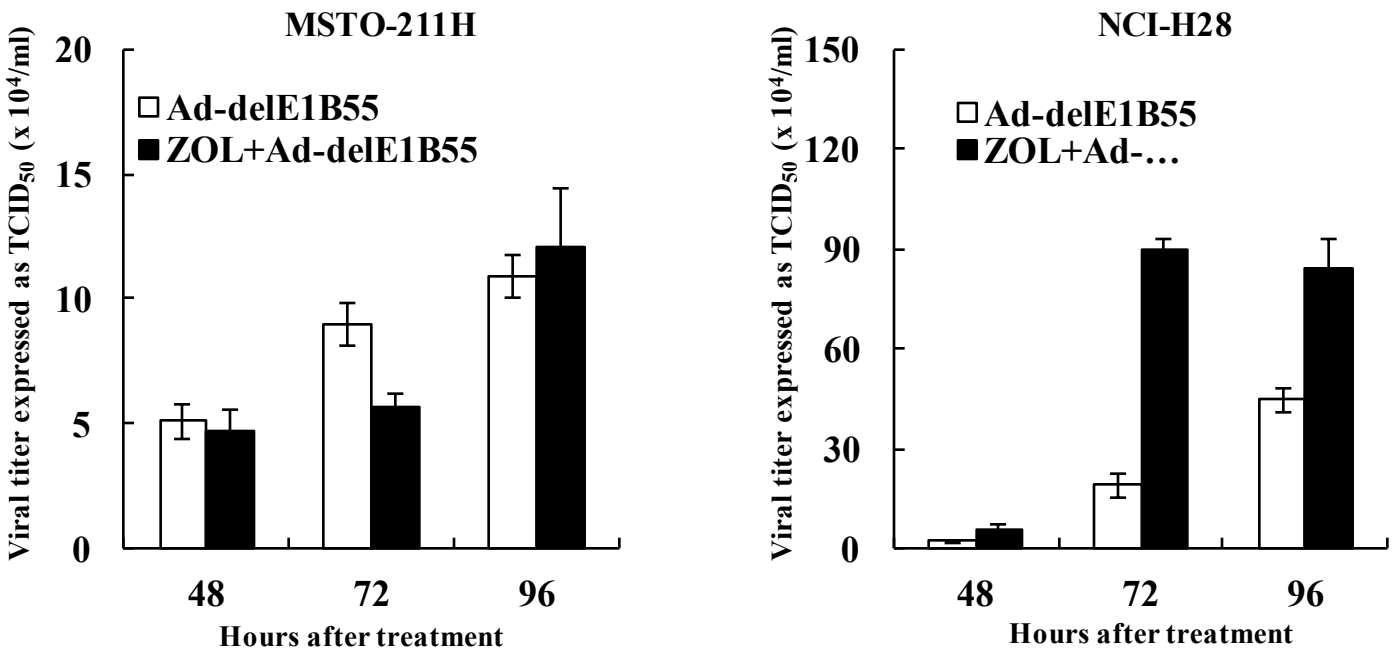
MSTO-211H
Ad-delE1B55
ZOL+Ad-delE1B55
Viral titer expressed as TCID50 (x 10^4/ml)
0
5
10
15
20
48
72
96
Hours after treatment
NCI-H28
Ad-delE1B55
ZOL+Ad-…
Viral titer expressed as TCID50 (x 10^4/ml)
0
30
60
90
120
150
48
72
96
Hours after treatment

BMC Cancer

平成 28 年 02 月 23 日　　投稿中